

# Simulink Modeling And Simulation Of A DC Motor Driven Pump Sprinkler Irrigation System

Anamekere Ime Jacob<sup>1</sup>

<sup>2</sup>Department of Electrical/Electronic and Computer Engineering, University of Uyo, Akwalbom, Nigeria.

Harrison Osasogie Edokpolor<sup>2</sup>

<sup>1</sup>Department of Electrical/Electronic Engineering Imo State Polytechnic, Umuagwo, Owerri, Nigeria

Victor Etop Sunday<sup>3</sup>

Department of Electrical/Electronic and Computer Engineering  
University of Uyo Akwa Ibom State Nigeria  
etop\_victor@yahoo.com

**Abstract—** In this paper, Simulink modeling and simulation of a DC motor driven pump sprinkler irrigation system is presented. The relevant transfer functions of the various system components were used to develop the Simulink models for the system. Then maize crop was selected for the simulation. The pump model was simulated for about 0.01 second and the continuous-time transfer function reacted with a very fast response time which reached a maximum flow rate of 25.86mm<sup>3</sup>/s in less than 0.004 second. The results show that the value of the motor armature resistance significantly affects the flow rate; the higher the motor armature resistance the lower the flow rate developed by the pump and vice versa. Also, there was need to introduce a controller into the overall plant system to boost the value of the flow rate to at least 1×10<sup>5</sup> mm<sup>3</sup>/s required to maintain maximum of 800 mm water layer from the sprinkler heads which was adequate for the root zone of maize crop.

**Keywords—** Water Pump, Sprinkler Irrigation, Sprinkler Head, DC Motor, Transfer Functions, Motor Armature Resistance

## I. INTRODUCTION

As the world population increases, there is need to improve on food production in order to meet the increasing demand [1,2]. While there has been different technologies that have been developed for enhanced food production, irrigation is one of the established viable means of improving crop yield, especially during dry season or in those areas where there is inadequate water supply [3,4,5].

Basically, irrigation is an artificial way of providing water to plants so as to meet the plants' water demand for effective growth and optimal yield [6,7,8,9]. Irrigation water can be delivered manually. However, over the years, pumped water irrigation system has become popular. In that case, electric motor-driven water pump is used to provide the irrigation water [10,11,12] which can be delivered to the plant using any of the available irrigation methods, such as basin, furrow, sprinkler and drip methods [13,14]. Whichever method is adopted, there is need to supply adequate water without water logging the farm.

Consequently, experts have developed different analytical models that can be used to evaluate the water requirement of plant, the nature of soil and its water holding capacity, the water supply flow rate of pumped water irrigation system and how these diverse factors are brought together to effectively meet the water need of the plant through an irrigation system [15,16,17,18,19,20]. In this paper, the Simulink modeling and simulation of a DC Motor driven pump sprinkler irrigation system is presented. The study utilizes the transfer function of the various subunits of the irrigation system to develop the Simulink models which are eventually simulated to evaluate the performance of the subunit and the entire irrigation system as well. The study in this paper is meant to examine to what extent a DC motor driven pump sprinkler irrigation system can meet the water requirement of a maize cop where the irrigation system does not have a controller for optimal performance. Specifically, the maximum water flow rate of the pump, the maximum volume of water pumped at a given time and the case study crop water requirement are examined to see whether the irrigation system can effectively satisfy the water demand of the crop. The study is relevant as it provides the basis for further studies on the use of various controllers for optimal water flow rate and adequate irrigation water supply to the crop.

## II. METHODOLOGY

### A. The Simulink Model For The DC Motor Driven Irrigation Pump

In this study, simulation models for DC motor driven centrifugal pump for sprinkler irrigation system is presented. The model takes in a DC voltage,  $V_a$ , as an input to the motor and the output is the flow rate,  $Q$ . Particularly, the Simulink model of the DC motor driven irrigation pump is based on the transfer function for the pump-motor relationship that yield voltage as input to the system and pump flow rate as output, as follows;

$$\frac{Q(s)}{V_a(s)} = \frac{K_m r m^3}{8LJ s^2 + (8LK_f + BLr m^3 + 8JR)s + (8RK_f + BRr m^3 + 8JK_b)} \quad (1)$$

The Simulink model of the transfer function is shown in Figure 1. When the values of the input parameters in Tables 1 are considered the transfer function model becomes;

$$\frac{Q(s)}{V_a(s)} = \frac{4.089 \times 10^6}{0.1433s^2 + 1.313 \times 10^4 s + 3.872 \times 10^6} \quad (2)$$

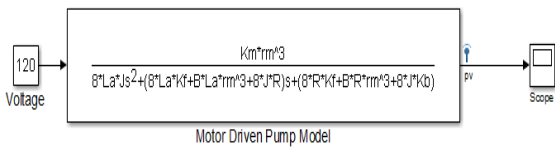


Figure 1: Transfer function model for DC motor driven centrifugal pump

Table 1: The simulation input parameters of the DC motor driven pump and the sprinkler

DC motor driven pump parameters		Pump and sprinkler model parameters	
Parameters	Values	Parameters	Values
Motor armature inertia	10.2kgmm <sup>2</sup>	Pump speed	1750rpm
Back emf constant	0.0283	Pump flow rate	1020000mm <sup>3</sup> /s
Viscous damping coefficient	5.8	Pump discharge pressure	0.51712N/mm <sup>2</sup>
Armature torque constant	2.83	Pump impeller exit blade angles	23degrees,45°
Armature coil inductance	0.00163H	Impeller inlet angles	90degree
Armature resistance	2.45ohms	Number of sprinkler heads	20
		Sprinkler nozzle constant	0.00443
		Irrigation application efficiency	85 percent
		Net irrigation depth	700mm
		Sprinkler spacing	2000mm
		Sprinkler lateral spacing	1500mm
		Effective water fraction	0.95
		Time to complete one irrigation	1day
		Hours of irrigation per day	5hours
		Water density	0.00000999kg/mm <sup>3</sup>

**B. The Simulink Model For The Soil Moisture Content**

The soil moisture,  $\theta$ , is a function of both time, t and location, z and the expression for the exact solution of the soil moisture is given as follows;

$$\theta(z, t) = \left[ \frac{\theta_d e^{\frac{\pi z}{2DL}}}{e^{\frac{c^2 t}{4D} + \frac{\pi^2 t}{L^2}}} - \frac{[(\theta_s - \theta_d) e^{\frac{\pi z}{2DL}} - \theta_d e^{-\frac{cL}{2D} + \frac{\pi}{2D} + \frac{\pi z}{2DL}}]}{\left( e^{-\frac{cL}{2D} - \frac{c^2 t}{4D} + \frac{\pi^2 t}{L^2}} - \frac{\pi}{2D} e^{-\frac{cL}{2D} + \frac{\pi^2 t}{L^2} + \frac{\pi}{2D}} \right)} \right] + \left[ \frac{[(\theta_s - \theta_d) e^{-\frac{\pi z}{2DL}} - \theta_d e^{-\frac{cL}{2D} + \frac{\pi}{2D} - \frac{\pi z}{2DL}}]}{\left( e^{-\frac{cL}{2D} - \frac{c^2 t}{4D} + \frac{\pi^2 t}{L^2}} - \frac{\pi}{2D} e^{-\frac{cL}{2D} + \frac{\pi^2 t}{L^2} + \frac{\pi}{2D}} \right)} \right] e^{-\frac{cz}{2D} - \frac{c^2 t}{4D} + \frac{\pi^2 t}{L^2}} \quad (2)$$

Where c is a constant defined as follows:

$$C = \frac{K_s}{\theta_s - \theta_d} \quad (3)$$

Where  $\theta$  is the soil moisture content, z represents the vertical distance from the soil surface downwards, t is time, A is the area of a cross section of the cylinder perpendicular to the direction of flow,  $K_s$  is the hydraulic conductivity when the soil becomes saturated with water,  $K_r$  is the relative hydraulic conductivity,  $\theta_d$  is moisture content when the soil is dry and  $\theta_s$  is the saturated moisture content, L is plant root zone from the phreatic surface, D is the soil water diffusivity, K is the hydraulic conductivity, q is the soil water flux density, H represents the total hydraulic head, and V is the volumetric overflow.

The soil moisture model in Equation (2) is modelled in Figure 2 and then programmed as a Simulink function and the codes extract is shown in Figure 3. This model is simulated with the parameters documented in Table 2.

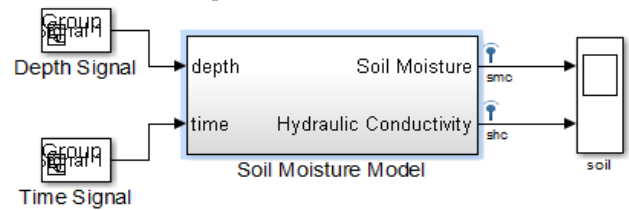


Figure 2: Simulink soil moisture model showing actual inputs and output

Table 2: Soil model sample parameters

Parameters	Values
Soil type	Clay
Hydraulic Diffusivity	0.5mm <sup>2</sup> /s
Saturated Hydraulic Conductivity	0.001mm/s
Soil moisture at dryness (wilting point)	20mm <sup>3</sup> H <sub>2</sub> O/mm <sup>3</sup> Soil
Soil moisture at saturation	100mm <sup>3</sup> H <sub>2</sub> O/mm <sup>3</sup> Soil

```
function [A,B,C,D1,Q,Se,K] =
Jacob_script1(L,D,Qs,Qd,Ks,c,z,t)
%% Analytical Approach to Automatic
Irrigation Control System
%% This thesis uses Richard's Equation of
water movement in unsaturated soils.
% The solution was developed using
separation of variables to the derived
% nonlinear homogeneous partial
differential equation

A = (Qd.*(exp(pi.*z./(2.*D.*L)))) ./ (exp((-
c^2.*t)/(4.*D)+(pi^2.*t)/(L^2)));
B = ((Qs-Qd)-Qd.*exp((-
c.*L)/(2.*D)+pi./(2.*D)).*exp((pi.*z)/(2
.*D.*L)));
C = (Qs-Qd).*exp((-pi.*z)/(2.*D.*L))-
Qd.*exp(((c.*L)/(2.*D)+(pi./(2.*D))-
(pi.*z)/(2.*D.*L)));
D1 = exp(((c.*L)/(2.*D))-
((c.^2.*t)/(4.*D))+((pi^2.*t)/(L.^2))-
pi./(2.*D))-exp(((c
.*L)/(2.*D))+((pi^2.*t)/(L.^2))+pi./(2.*
D)));
Q = (A-(B./D1)+(C./D1)).*exp(((c
.*z)/(2.*D))-
((c^2.*t)/(4.*D))+((pi^2.*t)/(L^2)));
% Calculate the true hydraulic conductivity
Se = (Q-Qd)/(Qs-Qd);
K = Ks.*Q/(Qs-Qd)-Ks.*Qd/(Qs-Qd);
%% END
```

Figure 3: The Simulink code for soil moisture content model

The soil moisture model is simulated for 2000 seconds with time and soil depth as varying basic inputs and volumetric moisture content growth and hydraulic conductivity as the output. This is to help visualize how well the model has been able to mimic the real soil water movement characteristics.

C. The Simulink Model For The Plant Water Uptake Process

The plant water uptake model is given as:

$$P_w = -\frac{K\mu}{\rho g g} \left[ \frac{p_r}{z} - \rho g g \right] - e^{-\frac{c^2 t}{4D} + \frac{\pi^2}{L^2} t} \quad (4)$$

Where  $\mu$  is the dynamic viscosity of the fluid,  $p_r$  is the root fluid pressure inside the xylem tubes,  $k$  is the hydraulic conductivity,  $z$  is the position along the root,  $\rho$  is water density,  $g$  is the acceleration due to gravity and  $P_w$  is the plant water uptake. The Simulink model for the plant water uptake is shown in Figure 4.

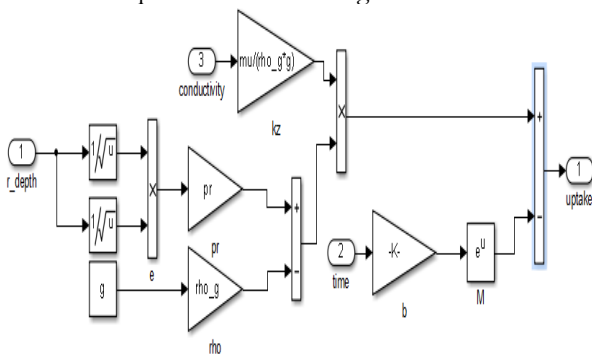


Figure 4: Simulink model for the plant water uptake

In order to simulate the model, there is need to link this unit to the soil moisture characteristic, called the true soil hydraulic conductivity, root zone depth and time. The Simulink model is given in Figure 5. The experiment was carried out for a period of 2 seconds using system parameters given in Table 3 and the result are presented under the results and discussion section.

Table 3: Plant water uptake process model parameters

Parameters	Values
Xylem tube fluid pressure	9000000000N/mm <sup>2</sup>
Radius of xylem tube vessel	0.0006mm
Number of functional xylem vessels	45
Index for different radius categories	2
Density of xylem fluid	0.000001kg/mm <sup>3</sup>
Dynamic viscosity	0.00000091kg/mm-s
Acceleration due to gravity	9810mm <sup>2</sup> /s

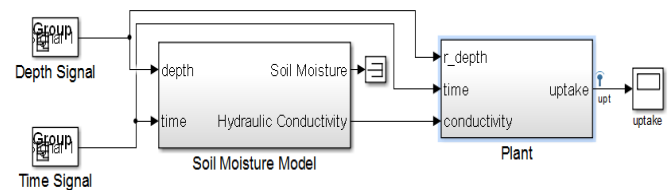


Figure 5: Plant soil moisture uptake model connected to soil moisture model

D. Simulation Of The Sprinkler Model

A sprinkler irrigation system was chosen to mimic precipitation (rainfall) which is one of the natural sources of water in the farm. In this work, 20 heads of sprinkler irrigation system were adopted for the experimental field, and were spaced as illustrated in Figure 6. The simulation was carried out with a first order transfer function presented in the transfer function in Equation (1) which is also modelled in Figure 7. The model consist of the flow rate coming from the pump as the input and the application depth as the output.

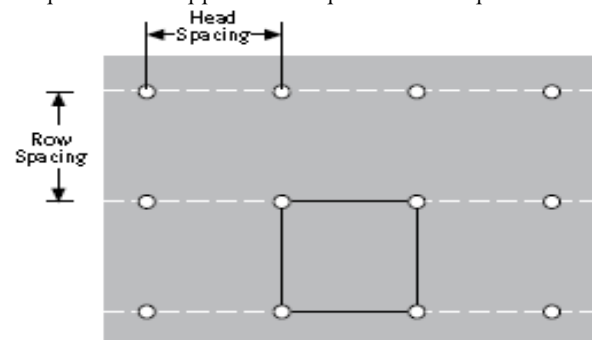


Figure 6: Sprinkler heads model and spacing

In the simulation, a100,000 mm<sup>3</sup>/s of water was channelled through the sprinkler head nozzle, and the precipitation and application rates were investigated. The

sprinkler head nozzle behaviour was simulated for 2000 seconds and the behaviour shows that regardless of the flow rate, the precipitation rate increases with time as follows;

$$\frac{d_g(s)}{Q_T(s)} = \frac{3600K_oA_r f T R_e \sqrt{P_s}}{(K_t d_n) s} \quad (5)$$

Where T is the hours of system operation per day, P<sub>s</sub> is the sprinkler pressure, f is time to complete one irrigation (days), A<sub>r</sub> is the sprinkler nozzle area, K<sub>t</sub> is coefficient for conversion of units, d<sub>n</sub> is net irrigation rate, R<sub>e</sub> is the fraction of water emitted by the nozzle that reaches the soil, taking into account the evaporative and wind losses.

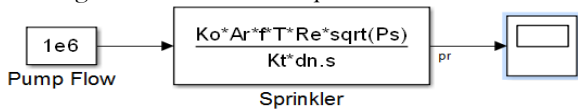


Figure 7: Simulink sprinkler head model

### E. Simulink Model Of The Integrated System Components

In control systems design, it is important to always couple the components models together in a way it is meant to work in real life. This is meant to determine if there will be any integration issues that may call for the redesign of the system or cause adjustments in the system parameters. Figure 8 is an overall plant model without incorporation of any controller. This shows the DC motor driven pump model taking in a DC input voltage of 120V and giving an output which is the water flow rate to the sprinkler head nozzle.

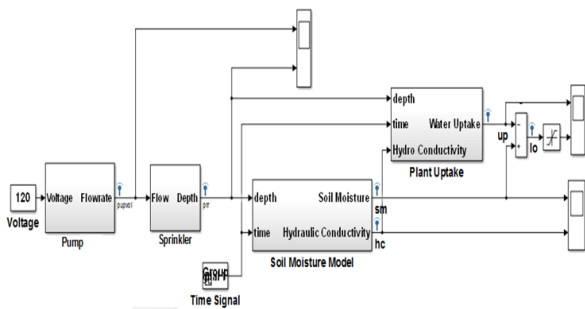


Figure 8: Integration of developed Simulink model

The sprinkler nozzle sprays the water droplets on the field (soil moisture model) which is denoted in the model as an application rate. The plant water uptake model now feeds from the soil moisture content and the soil moisture content depletion could be studied in order to develop a workable automatic controller for the system. The entire integrated system was simulated for 1500 seconds and its behaviour studied and the results are presented in the result and discussion section.

## III. RESULTS AND DISCUSSION

### A. Simulation Results Of The Motor Driven Centrifugal Irrigation Pump

For the simulation in Simulink, the DC motor driven pump parameters are as follows: motor armature inertia = 10.2kgmm<sup>2</sup>; back emf constant = 0.0283; viscous damping coefficient = 5.8; armature torque constant = 2.83; armature coil inductance = 0.00163 H and armature resistance = 2.45ohms. The simulation of the sprinkler irrigation system was carried out for maize crop. The pump model was simulated for about 0.01 second and the

continuous-time transfer function reacted with a very fast response time which reached a maximum flow rate of 25.86mm<sup>3</sup>/s in less than 0.004 second. The most influential parameter on the value of flow rate is the motor armature resistance, the higher its value the lower the flow rate developed by the pump and vice versa.

However, although the pump model exhibit a stable performance, the maximum supplied volume of water per unit time to the sprinkler is low. There was need to introduce a controller into the overall plant system to boost the value of the flow rate to at least 1×10<sup>5</sup>mm<sup>3</sup>/s required to maintain maximum of 800mm water layer from the sprinkler heads which was adequate for the root zone of maize crop.

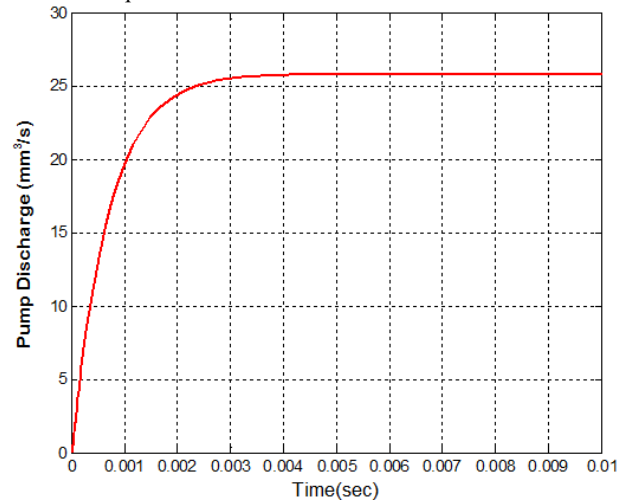


Figure 3: Pump maximum flow rate

The time and frequency domain responses of the pump were also checked by accessing the step response, impulse and frequency response plots. First, the step response of the entire system was computed and shown in Figure 4.

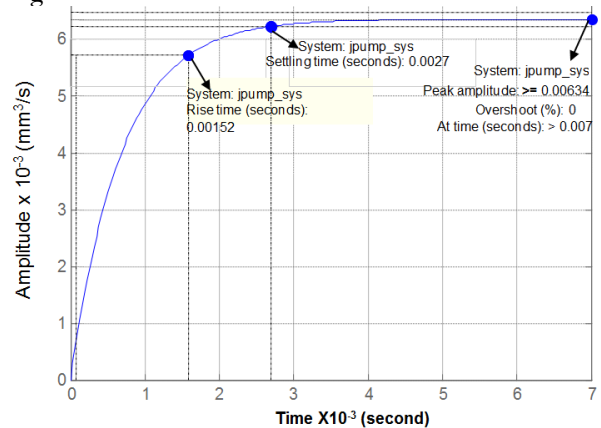


Figure 4 : Step response of pump model

The response of the model corresponds with the performance obtained with the flow characteristics of the pump. The system step response displayed is not chaotic, as such, the system has no internal delays which are evident from the smooth transition of the step plot with 0 % overshoot. A settling time of 0.0027second is fast enough for quick response of the pump system once the motor field circuit is energized. An equally low rise time of 0.0015second is also good for the unit as centrifugal pumps

are sensitive to discontinuous flow patterns within the impeller housing which most time results in cavitation and subsequent pump damage.

The open-loop impulse response of the continuous-time transfer function model of the pump simulated is shown in Figure 6. The results showed that the model registered peak amplitude of  $9.19\text{mm}^3/\text{s}$  within  $1.59 \times 10^{-7}$  second. Impulse response actually shows the response of the system to an impulse disturbance. In this case, the pump unit simply adjusted its dynamics which enabled the response to settle down at the envisaged value in just 0.0027 second, equal the step response settling time in Figure 5. This means that the system can easily regulate external disturbances such as voltage surges and hysteresis into the system without compromising the open-loop stability.

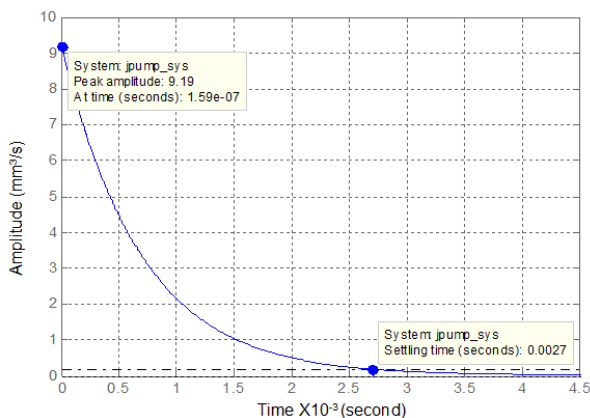


Figure 5: Impulse response of pump model

Frequency-domain analysis is vital tool for having clear understanding of stability and performance properties of control systems. It could also be seen as a steady-state response of a system to sinusoidal input test signal as frequency varies. The input signal and the output have the same response frequency but their magnitude and the phase of the signals differs. Adjusting frequency-domain characteristics such as gain margins, phase margins and bandwidth of the system can enable the designer to obtain satisfactory response.

From the result in Figure 6, the maximum value of the frequency response was found to be 471dB and occurred at the resonant frequency of  $1 \times 10^{-20}$  rad/s. It can be noticed that the amplitude of the bode plot does not oscillate at any point along the path which point to absence of resonant behaviour by the complex poles normally formed in closed-loop. In the same vein, the gain margins were found to be 111dB (closed-loop) at the same gain crossover frequency of  $2.75 \times 10^6$  rad/s. The results indicated that the closed-loop system exhibit more robustness and stability because its gain margin is wide enough. Also, phase margin of 64.3degrees at  $2.55 \times 10^3$  rad/s. This means that gain and phase margins could be varied from zero to their respective thresholds before the system starts losing stability.

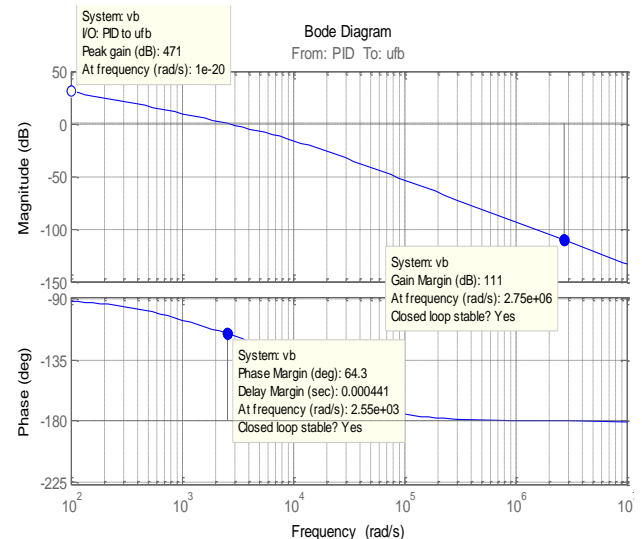


Figure 6: Frequency response of pump model

### B. Simulation Results Of The Sprinkler Head Model

The second most important subsystem of the entire plant is the sprinkler head model which is responsible for scattering the water flow from the pump into fine droplets over a specified land mass. Its model is a first order continuous-time model which was modelled to output a continuous precipitation rate over time. The sprinkler response is as shown in Figure 7.

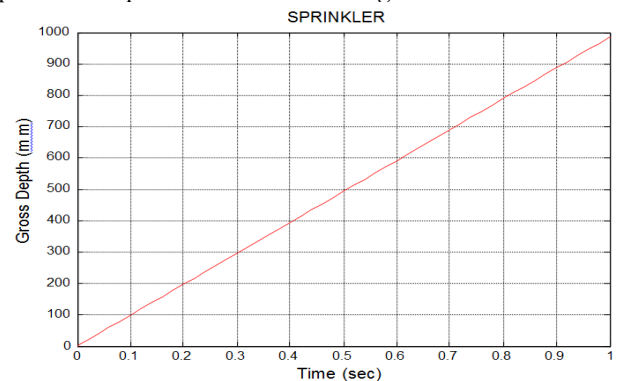


Figure 7: Sprinkler gross depth response with time

The gross depth increases linearly with time having received a constant flow rate of  $1 \times 10^6 \text{mm}^3/\text{s}$  through the sprinkler head. It is seen from the graph that at 0.9 second, the water supplied by the sprinkler to the soil has already reach the root depth of the plant and would tend to foster leaching. This scenario would hold true if the effect of wind was not considered as in this design. At this sprinkling gross depth, the corresponding precipitation rate is  $0.36 \text{mm}/\text{s}$ . This rate was quite slow and there was need to incorporate a PID controller within the loop to enhance the speed of application. The sprinkler precipitation rate will also be improved if its parameters are being varied especially the nozzle diameter.

### C. Simulation Results Of The Soil Moisture Model

The soil moisture model which takes in gross depth and time input signal was designed to output volumetric soil moisture content and hydraulic conductivity as shown in Figure 8.

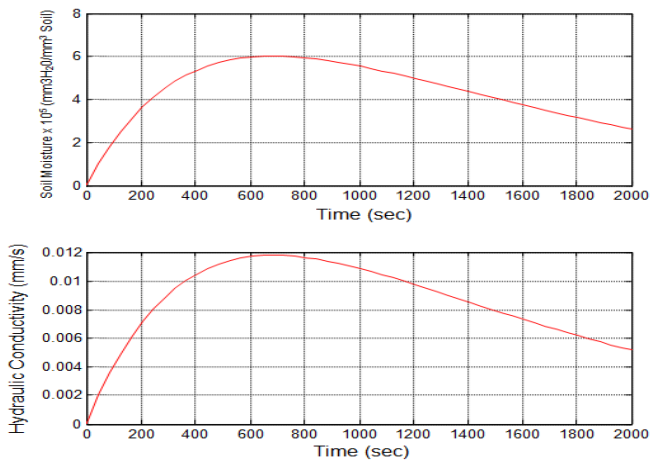


Figure 8: Soil moisture content model response

From upper subplot, the model recorded a maximum or saturated moisture content of  $6.0043 \times 10^5 \text{mm}^3 \text{H}_2\text{O}/\text{mm}^3 \text{Soil}$  and a corresponding saturated hydraulic conductivity of  $0.0118 \text{mm/s}$  within 700seconds (0.23hour) of simulation. This means that the soil under consideration would remain unsaturated until this time period is exceeded. The shapes of the soil moisture content and hydraulic conductivity look alike because the later depends on the former for its values. Beyond this time the growth began to fall showing that from that point onward the soil can no longer absorbed the water applied to it. This is the situation where soil swelling occurs if it's a purely clayey soil, possibility of soil surface runoff and plant nutrients leaching. The determination of the saturation point is very crucial in the design of the automatic controller for the irrigation system because this will serve as soil moisture sensor high set point while the maize plant documented wilting point will be considered as the sensor lower set point. It is noted that the response of this model is very fast, that is, the soil would reach its saturation in just 13.8minutes. As earlier seen in fastness of other models responses, it is of necessity to have at least one PID controller within the overall system closed-loop in order to further increase the response time to what could be possibly obtained in practice.

#### D. Simulation Results Of The Plant Water Uptake Model

The model inputs of the plant water uptake process are plant root depth or zone, the soil hydraulic conductivity and plant xylem cell hydraulic conductivity while the output is volumetric water uptake per cubed unit of soil. It is important to mention that how readily water flows through plant root cells and tissues is encapsulated in the term hydraulic conductivity. Hydraulic conductivity is especially important when water travels over long distances, such as across a stem, and where there are barriers to water flow, such as suberized layers of roots.

From the graph in Figure 9, it can be seen that plant water uptake exhibits a quadratic inverse proportionality where water travels faster at the beginning and slower as time progresses. At time just greater than zero, the plant draw high soil moisture of about  $4.3469 \times 10^5 \text{mm}^3 \text{H}_2\text{O}/\text{mm}^3 \text{Soil}$  which later starts decreasing gradually to a point that plant can no longer absorb the moisture. The rate of decrease also depends

immensely on the rate of water transpiration and evapotranspiration from the plant leaves surfaces. However, there was no consideration made on these aspects, and it is beyond the scope of the work.

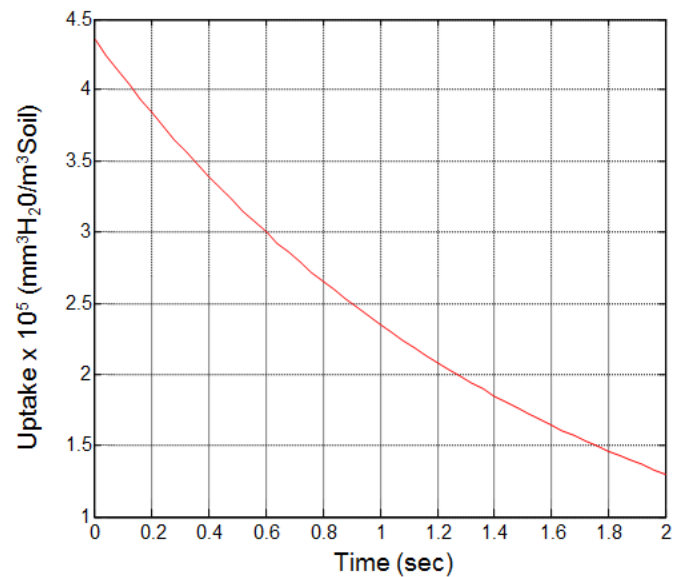


Figure 9: Plant water uptake process model response

#### E. Simulation Results Of The Integrated System Model

There are always some issues arising when integrating the subsystems of a complex system of this nature. The integration usually causes dynamics in one subsystem to further create dynamics in others. The pump and sprinkler responses in the overall system is given in Figure 10.

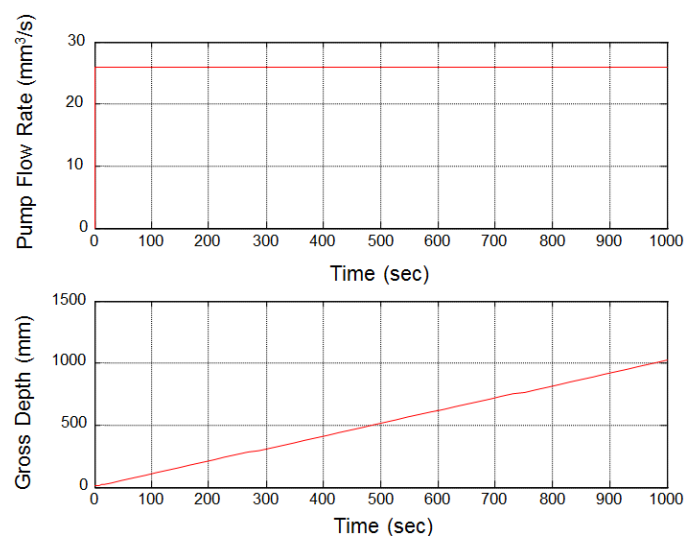


Figure 10: Pump and sprinkler responses in the overall system

From the previous sections 3.1, 3.2 and 3.3, the response of the pump flow rate was exactly as the one shown in Figure 4 but the time for the system flow to stabilize at the  $25.86 \text{mm}^3/\text{s}$  was much shorter. Also, the same results were obtained for the sprinkler gross depth. The integration in this case only affected the pump and sprinkler subsystems in terms of their response time, which is much longer than when these were simulated

individually. However, this is not the case for the soil moisture growth model as can be seen in Figure 11.

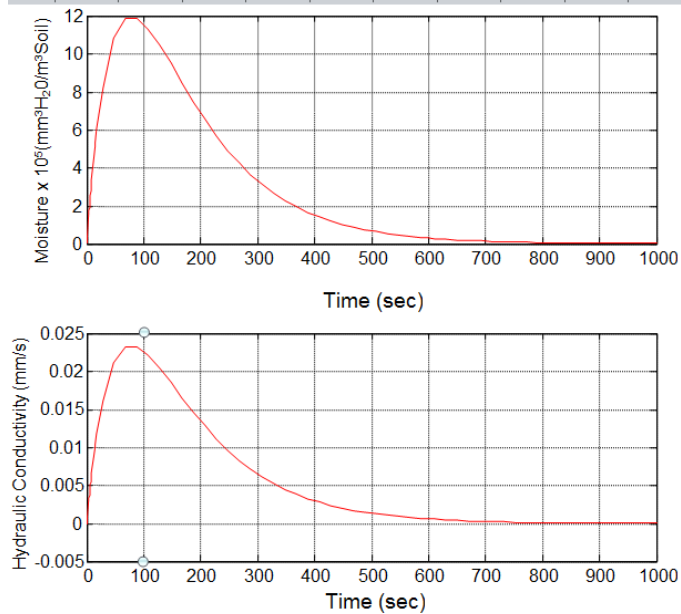


Figure 11: Soil moisture subsystem response in overall system

Although the response here seems faster than when it was simulated individually, taking less than 100 seconds to attain the saturated soil moisture content, the recorded value was quite higher as  $1.184 \times 10^6 \text{ mm}^3 \text{ H}_2\text{O} / \text{mm}^3 \text{ Soil}$  and a corresponding maximum hydraulic conductivity of  $0.0232 \text{ mm/s}$ . This is the true system behaviour that was taken into consideration before the automatic control logic was finally developed. The plant water uptake subsystem also experienced slight changes in its response as a result of the corresponding change that occurred in the other subsystems. As earlier recorded in Section 3.4, the model in its standalone simulation showed that the plant absorbed a maximum of  $4.3469 \times 10^5 \text{ mm}^3 \text{ H}_2\text{O} / \text{mm}^3 \text{ Soil}$  compared with  $6.0 \times 10^5 \text{ mm}^3 \text{ H}_2\text{O} / \text{mm}^3 \text{ Soil}$  in the overall system. However, it is noted that the water uptake process behaviour remains unchanged and showed an inversely proportional profile.

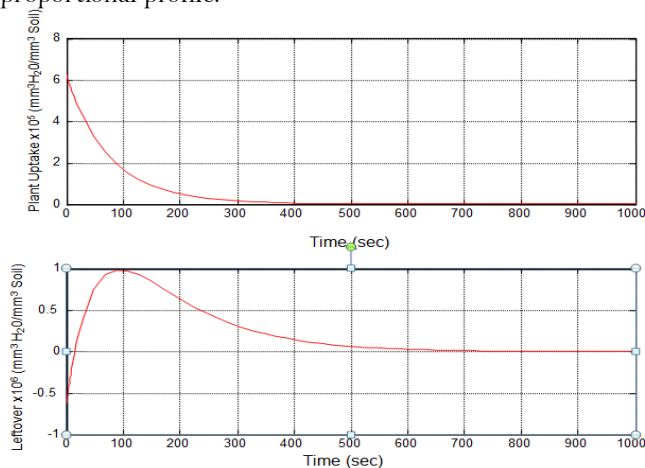


Figure 12: Plant water uptake subsystem response in overall system

The second subplot in Figure 12 was introduced to show how much the soil water has been depleted as the plant draws. This is the reason why its profile is a replica of the soil moisture growth patterns. The peak of the graph showed a maximum value of  $9.887 \times 10^5 \text{ mm}^3 \text{ H}_2\text{O} / \text{mm}^3 \text{ soil}$  which indicated that within this period, the plant has absorbed  $1.9573 \times 10^5 \text{ mm}^3 \text{ H}_2\text{O} / \text{mm}^3 \text{ soil}$  of the soil moisture.

#### IV. CONCLUSION

In this paper, a DC motor driven centrifugal pump for sprinkler irrigation system is modeled and simulated using Simulink software. The model is based on relevant transfer functions of the various system components. The pump-motor transfer function has voltage as input to the system and the pump flow rate as the output. Also, the soil moisture is modeled as a function of both time and location. Also, modeled are the plant water uptake process and the sprinkler head nozzle behaviour. The simulation is carried out for maize crop. The simulations were conducted for the individual system components and then the system components are integrated and simulated. Results show that although the pump model exhibited a stable performance, the maximum supplied volume of water per unit time to the sprinkler is low. Therefore, it requires a controller to maintain the pump flow rate at the value that is appropriate for the case study crop.

#### REFERENCE

1. Mozumdar, L. (2012). Agricultural productivity and food security in the developing world. *Bangladesh Journal of Agricultural Economics*, 35(454-2016-36350), 53.
2. Tilman, D., Balzer, C., Hill, J., & Befort, B. L. (2011). Global food demand and the sustainable intensification of agriculture. *Proceedings of the National Academy of Sciences*, 108(50), 20260-20264.
3. El Afandi, G., Khalil, F. A., & Ouda, S. A. (2010). Using irrigation scheduling to increase water productivity of wheat-maize rotation under climate change conditions. *Chil J Agric Res*, 70(3), 474-484.
4. Greaves, G. E., & Wang, Y. M. (2017). Identifying irrigation strategies for improved agricultural water productivity in irrigated maize production through crop simulation modelling. *Sustainability*, 9(4), 630.
5. Morison, J. I. L., Baker, N. R., Mullineaux, P. M., & Davies, W. J. (2007). Improving water use in crop production. *Philosophical Transactions of the Royal Society B: Biological Sciences*, 363(1491), 639-658.
6. Bodner, G., Nakhforoosh, A., & Kaul, H. P. (2015). Management of crop water under drought: a review. *Agronomy for Sustainable Development*, 35(2), 401-442.

7. Evans, R. G., & Sadler, E. J. (2008). Methods and technologies to improve efficiency of water use. *Water resources research*, 44(7).
8. Semananda, N., Ward, J., & Myers, B. (2018). A Semi-Systematic Review of Capillary Irrigation: The Benefits, Limitations, and Opportunities. *Horticulturae*, 4(3), 23.
9. Jury, W. A., & Vaux, H. (2005). The role of science in solving the world's emerging water problems. *Proceedings of the National Academy of Sciences*, 102(44), 15715-15720.
10. Jin, C., Wang, B., Jiang, D., & Jiang, W. (2011). Energy Conversion Stage Design of Solar Water Pump in a Nanofiltration System. *Energy Procedia*, 12, 1049-1056.
11. Hassan, W., & Kamran, F. (2018). A hybrid PV/utility powered irrigation water pumping system for rural agricultural areas. *Cogent Engineering*, 5(1), 1-15.
12. Chandel, S. S., Naik, M. N., & Chandel, R. (2015). Review of solar photovoltaic water pumping system technology for irrigation and community drinking water supplies. *Renewable and Sustainable Energy Reviews*, 49, 1084-1099.
13. Tagar, A., Chandio, F. A., Mari, I. A., & Wagan, B. (2012). Comparative study of drip and furrow irrigation methods at farmer's field in Umarkot. *World Academy of Science, Engineering and Technology*, 69, 863-867.
14. Bryla, D. R., Dickson, E., Shenk, R., Johnson, R. S., Crisosto, C. H., & Trout, T. J. (2005). Influence of irrigation method and scheduling on patterns of soil and tree water status and its relation to yield and fruit quality in peach. *HortScience*, 40(7), 2118-2124.
15. Lee, J. L., & Huang, W. C. (2014). Impact of climate change on the irrigation water requirement in Northern Taiwan. *Water*, 6(11), 3339-3361.
16. Greaves, G., & Wang, Y. M. (2016). Assessment of FAO AquaCrop model for simulating maize growth and productivity under deficit irrigation in a tropical environment. *Water*, 8(12), 557.
17. Souza, J. L. M. D., Gerstemberger, E., Gurski, B. C., & Oliveira, R. A. D. (2015). Adjustment of water-crop production models for ratoon sugarcane. *Pesquisa Agropecuária Tropical*, 45(4), 426-433.
18. Flörke, M., Lapola, D. M., Schaldach, R., Voß, F., & Teichert, E. (2010). Modelling historical and current irrigation water demand on the continental scale: Europe. *Advances in Geosciences*, 27, 79-85.
19. Seflek, A., & Çarman, K. (2010). A design of an expert system for selecting pumps used in agricultural irrigation. *Mathematical and Computational Applications*, 15(1), 108-116.
20. Fleming, R. P. (2016). Automatic sprinkler system calculations. In *SFPE Handbook of Fire Protection Engineering* (pp. 1423-1449). Springer, New York, NY.